


 Cite this: *RSC Adv.*, 2017, 7, 32777

# Fabrication of phytic acid-modified wheat straw platform and its pH-responsive release performance for the pesticide imidacloprid

 Peishan Qin,<sup>a</sup> Xiaohui Xu,<sup>b</sup> Yi Cai,<sup>b</sup> Bo Bai,<sup>b</sup> \*<sup>ab</sup> Honglun Wang<sup>a</sup> and Yourui Suo<sup>a</sup>

For the effective utilization of pesticides and the treatment of abundant waste wheat straw (WS) resources, an eco-friendly composite PA-WS platform was prepared by modification of WS with phytic acid (PA). The structure and morphology of the synthesized products were characterized via SEM, FTIR, and zeta surface potential analyses. Elemental analysis and X-ray photoelectron spectroscopy (XPS) were used to determine the degree of substitution (DS) and degree of surface substitution (DSS). The evaluation of the release properties of PA-WS@IM showed that the release of imidacloprid (IM) molecules could be controlled via a pH-sensitive dynamic chemical bond. The release efficiency of IM was enhanced with a decrease in pH and the release efficiency achieved a maximum (85.29%) at pH 2. The release efficiency of IM in a solution of Ca<sup>2+</sup> ions was higher than in the solution of Na<sup>+</sup> ions, while Fe<sup>3+</sup> ions aqueous solutions had no significant influence. Due to its controllable release, cost-effectiveness, reusability of a resource and eco-friendly preparation, it is believed that PA-WS@IM may have potential application in agriculture fields to enhance the utilization efficiency of pesticides and improve the comprehensive utilization of agriculture resources.

 Received 18th April 2017  
Accepted 12th June 2017

DOI: 10.1039/c7ra04354f

[rsc.li/rsc-advances](http://rsc.li/rsc-advances)

## 1. Introduction

Pesticides, as essential chemical reagents to control the existence or growth of weeds, pests and plant diseases, make major contributions to boost the world's crop yields and supplies.<sup>1</sup> Unfortunately, only a very small amount of an applied pesticide actually reaches its target site, and up to 90% of a pesticide is transferred into the environment through volatilization, decomposition, leaching and migration, leading to serious damage to the environment, ecology and economy.<sup>2,3</sup> In order to overcome this application restriction, the tactic of controlled stimuli-responsive release, namely, by gradually delivering the preloaded active ingredients to a targeted surface in a designated manner, is becoming a feasible and effective way to alleviate the harm of pesticide residues.<sup>4,5</sup> In particular, the preparation of sustained released systems with pH sensitivity performance has been frequently reported in the cargo delivery domain.<sup>6</sup> For example, Chen *et al.*<sup>7,8</sup> reported a pH-responsive sustained release system of chlorpyrifos/copper(II) Schiff base mesoporous silica. Sheng *et al.*<sup>9</sup> successfully developed a hydrazone bond induced hydrogel with a pH-responsive controlled avermectin-release pattern. Jia *et al.*<sup>10</sup> demonstrated

that the pesticide release performance of polydopamine-coated avermectin microcapsules can be tuned by changing the pH of the medium. However, it is very difficult to achieve practical applications of these formulations since the required agents are expensive, non-renewable or non-degradable, and even their preparation is somewhat intricate and requires harsh reaction conditions in some cases. Therefore, it is extremely significant to obtain a cost-effective and controllable pesticide delivery system based on raw materials that are very inexpensive, renewable, biodegradable and environmentally friendly.

Wheat straw, as a by-product of grain crops, is an important biological resource in the crop production system.<sup>11–13</sup> Thus far, the abundant wheat straw has been largely under-utilized and is mainly buried and discarded outside,<sup>14</sup> discharging millions of tonnes of carbon dioxide and carbon monoxide. This is not only a huge waste of a natural resource, but also releases serious pollution to the environment.<sup>15,16</sup> Notably, wheat straw possesses several natural advantages including being very inexpensive, incredibly abundant, completely biodegradable, and clearly renewable. More importantly, the main constituents of wheat straw are cellulose (32.1%), hemi-cellulose (29.2%) and lignin (16.4%), which contain hydroxyl, ketone, aldehyde, or carboxylic groups.<sup>17–19</sup> Due to the existence of these functional groups, wheat straw can be easily modified through esterification, etherification and co-polymerization. For instance, citric acid,<sup>20</sup> acrylic acid,<sup>21</sup> cationic surfactant,<sup>22</sup> and poly-ethyleneimine<sup>23</sup>-modified wheat straw have been reported as low-cost adsorbents for the removal of metal ions and dyes.

<sup>a</sup>State Key Laboratory of Plateau Ecology and Agriculture (Qinghai University), Xining, 810001, P. R. China. E-mail: baibochina@163.com; Fax: +86 29 82339961; Tel: +86 29 82339052

<sup>b</sup>College of Environmental Science and Engineering, Chang'an University, Xi'an, 710054, P. R. China



Hereby, considering its natural merits as well as the satisfactory adsorption capacity after modification, wheat straw may act as large-volume feedstock that can be used to potentially construct pH-responsive formulations for controlling pesticide release. However, the synthesis of pesticide release platforms using wheat straw as the raw material has been rarely reported.

Based on the above considerations, in the present study we first fabricated a pH-controlled pesticide release carrier *via* grafting phytic acid onto the surface of WS. The structure of the sample was characterized by FTIR and SEM, and its mechanism of formation was proposed. Imidacloprid (IM),<sup>24</sup> accounting for 11–15% of the total insecticide market, was chosen as a model pesticide to evaluate the loading and pH-responsive release properties of the PA-WS carrier. As expected, the obtained PA-WS product exhibits sensitive release traits for IM in response to changes in the pH. In addition, the present route can also be extended to the synthesis of various pH-sensitive platforms based on other natural cellulosic resources, which may have potential applications in agricultural or industrial areas because of their cost-effectiveness, simple preparation and practical applicability.

## 2. Experimental

### 2.1 Materials

The wheat straw used in this study was collected from suburban farmland in Xi'an (Shanxi China). Imidacloprid (IM, 95.3%), phytic acid (PA, 70 wt% in H<sub>2</sub>O), urea, dimethylformamide (DMF), ethyl alcohol, sodium hydroxide, and hydrochloric acid were purchased from Xi'an Chemical Reagent Factory (Shanxi, China) and used without further purification.

### 2.2 Preparation of wheat straw

Raw wheat straw powder (20 g) was dispersed in deionized water (1000 mL) in a beaker and then placed in a forced air oven to dehydrate at 80 °C for 6 h after a few minutes of mechanical stirring, and the liquid was filtered off. The filter residue was transferred into a beaker with 15% sodium hydroxide solution in a water bath and then stirred and heated at 70 °C for 1 h.<sup>25</sup> After that, the wet wheat straw powder was washed with ethanol and distilled water three times each to remove any residual solutions.

### 2.3 Preparation of phytic acid modified wheat straw

PA-WS was synthesized using the following procedure:<sup>26</sup> typically, wheat straw (2 g) was dispersed in DMF (30 mL) in a beaker. Then, phytic acid (2.1 mL) and carbamide (1.2 g) were poured into the beaker. After 30 min of mechanical stirring, the mixture was transferred to a reaction kettle and placed in a forced air oven. The oven temperature was adjusted to the desired level (40–120 °C) and the mixture was allowed to react for 5 h. After that, the reaction products were washed 3 times with distilled water. Finally, the modified wheat straw product was dried in a forced air oven at 50 °C.

### 2.4 Characterizations

The morphologies of WS, PA-WS and PA-WS@IM were observed using scanning electron microscopy (SEM), on a Hitachi S-4800 scanning electron microscope at an accelerating voltage of 15 kV, and an optical microscope (MA 2001). The Fourier transform infrared (FTIR) spectra of samples were obtained as KBr disks on a Thermo Nexus 470 FTIR spectrometer. XPS measurements were carried out on a Kratos AXIS 165 electron spectrometer. An elemental analyzer (Heraeus Co., Germany) was used to determine the elemental composition of the PA-WS composite.

### 2.5 Zeta potential

The pH of zero point charges (pH<sub>PZC</sub>) of the WS, PA-WS and PA-WS@IM samples were measured with the following procedures according to the literature:<sup>27</sup> herein, 50 mL of NaCl solution (0.01 mol L<sup>-1</sup>) was placed into a 250 mL beaker. The original pH value of the solution was adjusted successively between 2.0 and 12.0, and 0.1 g samples were added to the beaker. Thereafter, the beakers were filled with nitrogen gas, to remove the effect of CO<sub>2</sub> (a composition of the air) on the pH change, and then sealed and shaken at 313.15 K. After 48 h, the final pH was measured, and the ΔpH (final pH – original pH) was plotted against the original pH value. The pH<sub>PZC</sub> of samples was the pH at which the curve crossed the line of ΔpH = 0.

### 2.6 Determination of the DS and DSS

The content of carbon, hydrogen, nitrogen and oxygen in the unmodified WS and PA-WS samples was measured using elemental analysis to determine the degree of substitution (DS). The DS, which designates the average number of phosphate groups on each anhydroglucose unit, can be calculated according to the following equation:<sup>28</sup>

$$DS = \frac{6 \times M_C - M_{AGU} \times \% C}{M_{\text{ester grafted}} \times \% C - M_{C, \text{ester grafted}}} \quad (1)$$

where % C represents the relative carbon content in the sample, and  $M_{AGU}$  and  $M_{\text{ester grafted}}$  correspond to the molecular mass of the anhydroglucose unit and the grafted ester, respectively.  $M_{C, \text{ester grafted}}$  and  $M_C$  are the carbon molecular weight of the grafted moieties and anhydroglucose unit, respectively.

The degree of surface substitution (the number of phosphate groups per glucose unit, DSS) can be calculated directly from the surface P mass concentration, derived from atomic concentrations obtained from the XPS survey scans. Based on Andresen *et al.* and Missoum *et al.*, the DSS can be defined as follows:<sup>29,30</sup>

$$DSS = \frac{M_{AGU} \times \chi}{100 \times M_P - \chi \times M_{\text{grafts}}} \quad (2)$$

where  $\chi$  is the mass concentration of P,  $M_{AGU}$  is the molecular mass of one anhydroglucose unit (162.14 g mol<sup>-1</sup>) and  $M_P$  and  $M_{\text{grafts}}$  are the molecular weight of P and the grafted PA moieties (660.4 g mol<sup>-1</sup>), respectively.



## 2.7 pH-dependent IM release tests

The release properties of IM were determined at different pH values and ionic strengths of deionized water. Specifically, 0.1 g of PA-WS@IM was weighed accurately and added to 100 mL of deionized water with the pH values range of 2–10. Using the same method, PA-WS@IM was added to 100 mL of deionized water containing  $\text{Na}^+$ ,  $\text{Ca}^{2+}$  and  $\text{Fe}^{3+}$  cations ( $0.1 \text{ mmol L}^{-1}$ ). After 2 h of mechanical stirring, the concentration of IM in the mixtures was determined using UV-VIS spectroscopy.

## 3. Results and discussion

### 3.1 The formation and characterization of PA-WS and PA-WS@IM

The PA@WS pesticide release system was synthesized *via* grafting phytic acid onto the surface of WS. The detailed fabrication process used to prepare PA@WS and the mechanism of IM release are illustrated in Scheme 1.

The fabrication of the PA-WS composite began with the pretreatment of raw WS to eliminate hemicellulose, lignin, and other various ashes covering cellulose in wheat straw. After the pretreatment process, the reactivity of the raw lignocellulosic materials could be greatly increased because more cellulose-containing hydroxyl groups were exposed to the reaction reagents, making the subsequent grafting reaction much more easy.<sup>31</sup> In the subsequent procedure, when WS was dropped into a solution of PA, the hydroxyl groups ( $-\text{OH}$ ) of WS cellulose could couple with the phosphate moieties ( $-\text{H}_2\text{PO}_4$ ) in PA *via* an esterification reaction, implanting numerous PA molecules onto the surface of WS (step 1). On these grounds, the PA-WS composite, which possesses higher chemical reactivity and higher-level active sites compared with the naked WS substrates, was constructed, facilitating the binding of IM molecules onto the exposed surface of the WS substrate. In the following adsorption test (step 2), using PA as a chemical

bridge, the PA-WS platform was able to capture numerous IM molecules through covalent and non-covalent interactions including hydrogen-bonding interactions, van der Waals forces and electrostatic interactions. After reaching adsorption saturation, the PA-WS platform full of IM was dispersed into an acidic solution to realize the pH-controlled release of pesticides upon changing the level of acidity or alkalinity in the surrounding medium (step 3). Overall, the obtained PA-WS composite has been demonstrated to be a simple but effective pesticide reservoir with pH sensitivity, low-cost, simple preparation and practical applicability.

To illustrate the successful synthesis of PA-WS@IM, FT-IR spectroscopy was employed to characterize the WS, PA-WS@IM and PA-WS samples at different temperatures ( $60$ – $120^\circ\text{C}$ ), as presented in Fig. 1. In Fig. 1(a), the strong and broad band at  $3374 \text{ cm}^{-1}$  (O–H and N–H stretching vibrations),  $2931 \text{ cm}^{-1}$  (C–H stretching vibrations), and  $1060 \text{ cm}^{-1}$  (C–O–C stretching vibrations) were the characteristic absorption peaks

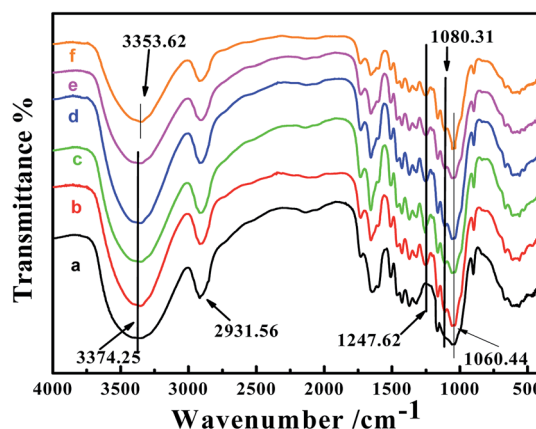
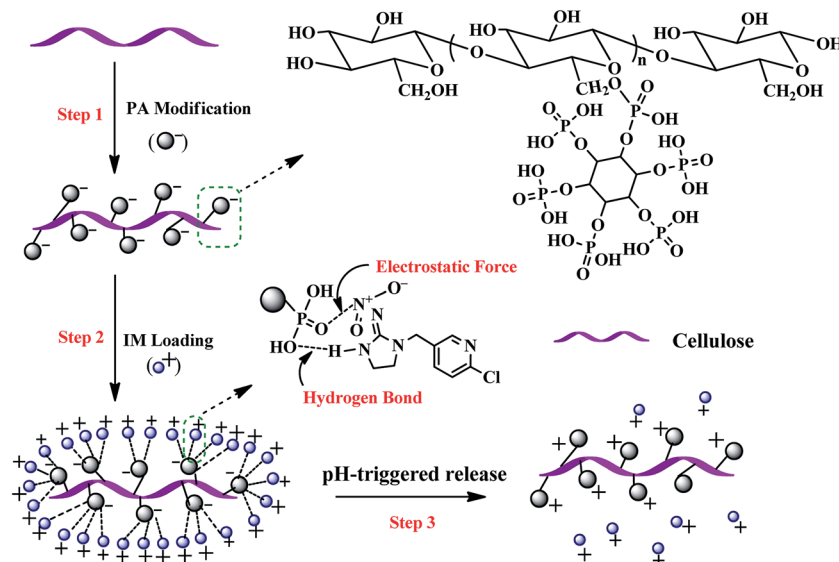


Fig. 1 The FT-IR spectra of WS (a), PA-WS at different temperatures varying from  $60^\circ\text{C}$  to  $120^\circ\text{C}$  (b–e) and PA-WS@IM (f).



Scheme 1 The proposed mechanism for the formation of the PA-WS composite and its pH-triggered release of IM.



of wheat straw.<sup>32,33</sup> In the IR spectrum of PA-WS, shown in Fig. 1(b–e), all the absorption bands of WS were maintained, and two strong peaks occurred at 1247  $\text{cm}^{-1}$  and 1080  $\text{cm}^{-1}$  corresponding to the stretching vibrations of P=O and P–OH, respectively.<sup>34</sup> These changes indicate the participation of the –OH groups in WS cellulose in the grafting with PA *via* an esterification reaction. Following the subsequent IM adsorption step, the peak at 3374  $\text{cm}^{-1}$  was shifted to 3353  $\text{cm}^{-1}$ , as shown in Fig. 1(f), due to the strengthening of the N–H stretching vibrations, indicating that IM was successfully adsorbed onto PA-WS. Overall, it can be concluded that numerous phosphate functional groups were introduced onto the WS surface *via* the chemical reaction between phytic acid and WS, which were available for binding the IM molecules onto the surface of PA-WS.

The successful grafting of phytic acid onto the WS substrate was also quantitatively verified by determining the amount of active functional groups since the amount of active functional groups on the PA-WS substrate plays an extremely decisive role in pesticide loading. In the present experiment, we have found that the grafting rate of PA-WS could be precisely controlled and adjusted using the reaction temperature. The theoretical and experimental data and the DS values obtained from the elemental analysis of the unmodified WS and PA-WS samples are presented in Table 1. It is clear in Table 1 that the temperature has a great influence on the degree of substitution grafting rate. The degree of substitution increased as the temperature ranged from 40 °C to 80 °C, while the DS value decreased rapidly upon a further increase in the temperature. A higher temperature favored a higher reaction rate between PA and the hydroxyl groups in WS because the diffusion of PA molecules was enhanced. Therefore, the degree of substitution increased upon increasing the temperature from 40 °C to 80 °C, and the maximum grafting rate at 80 °C was 0.26. However, the DS value decreased rapidly on exceeding 80 °C and reached a minimum (0.15) at 120 °C because some side reactions, including the degradation of some of the ester groups and oxidation of the hydroxyl groups in the sample, occurred at higher temperatures. All of these results suggest that it is more effective to increase the active sites in the PA-WS composite by fixing PA onto the WS surface, and 80 °C was selected to perform the subsequent IM adsorption experiments. For the quantitative evaluation of the

DSS of WS, the surface composition of unsubstituted and phosphorylated WS was examined by XPS, and the results are illustrated in Fig. 2. The WS spectrum only showed O 1s, N 1s and C 1s peaks, at 533 eV, 400 eV and 285 eV, respectively. In the spectrum of the PA-WS sample, two additional peaks occurred at 190 eV and 134 eV, corresponding to P 2s and P 2p, respectively, demonstrating the presence of P on the WS surface. The atomic compositions and the DSS values calculated from the P mass concentrations based on the relative peak areas in the survey scans of the investigated samples are summarized in Table 2. As can be seen, the number of grafted PA moieties on the WS surface increased as the reaction temperature was increased. However, when the temperature exceeded 80 °C, a substantial drop in the P content was observed, which was in agreement with the elemental analysis discussed above.

The PA anchored on the WS surface can be further verified by optical microscopy and SEM images. The surface topographies of the WS, PA-WS and PA-WS@IM samples were visualized by SEM and optical microscopy, and the images are shown in Fig. 3(a–c) and (d–f), respectively. As Fig. 3(a) and (d) show, while some flaws were made from the mechanical excitation, the surface morphology of WS was mainly smooth like sticks. The image, illustrated in Fig. 3(d), indicated that WS has a tubular structure.<sup>35</sup> After the grafting reaction with PA, the surface became rough as shown in Fig. 3(b) and (e). This indicated that after the reaction, PA was anchored onto the cellulose skeleton, leading to a porous and rougher surface of wheat straw.<sup>36</sup> These changes of the WS surface had a positive effect on the adsorption of IM by increasing the surface area for IM binding. Compared with PA-WS, the PA-WS@IM sample had no significant changes in its surface appearance, as exhibited in Fig. 3(d). In summary, the introduction of negatively charged phosphate groups endowed the PA-WS with much more IM-absorption sites than that of native WS, facilitating the loading and release of pesticides.

Based on the above analysis, it can be proposed that the wheat straw substrate and phytic acid modifier in the pH-triggered pesticide delivery system play extraordinarily important roles. In terms of WS, the substantial functional groups

**Table 1** Determination of the degree of substitution for PA-WS based on the elemental analysis data

Sample	Experimental values			Corrected values	
	% C	% H	% O	% O	DS
WS	43.71	5.30	49.79	49.38	—
PA-WS 40 °C	42.55	5.29	50.52	50.11	0.18
PA-WS 60 °C	42.57	5.43	50.30	50.89	0.23
PA-WS 80 °C	41.97	5.31	51.70	51.29	0.26
PA-WS 100 °C	41.74	5.44	50.12	50.71	0.21
PA-WS 120 °C	42.82	5.55	50.71	50.30	0.15

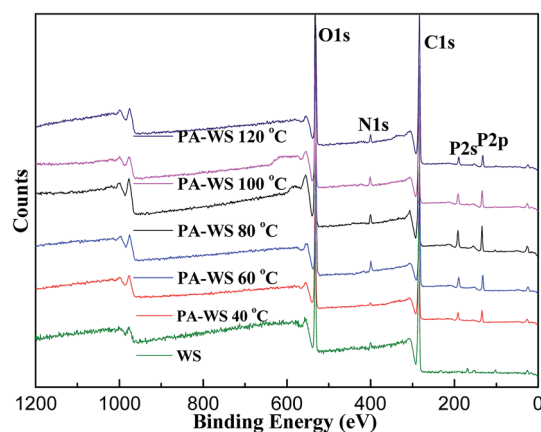


**Fig. 2** The XPS low-resolution survey spectra of unmodified WS and PA-WS at various temperatures (40–120 °C).



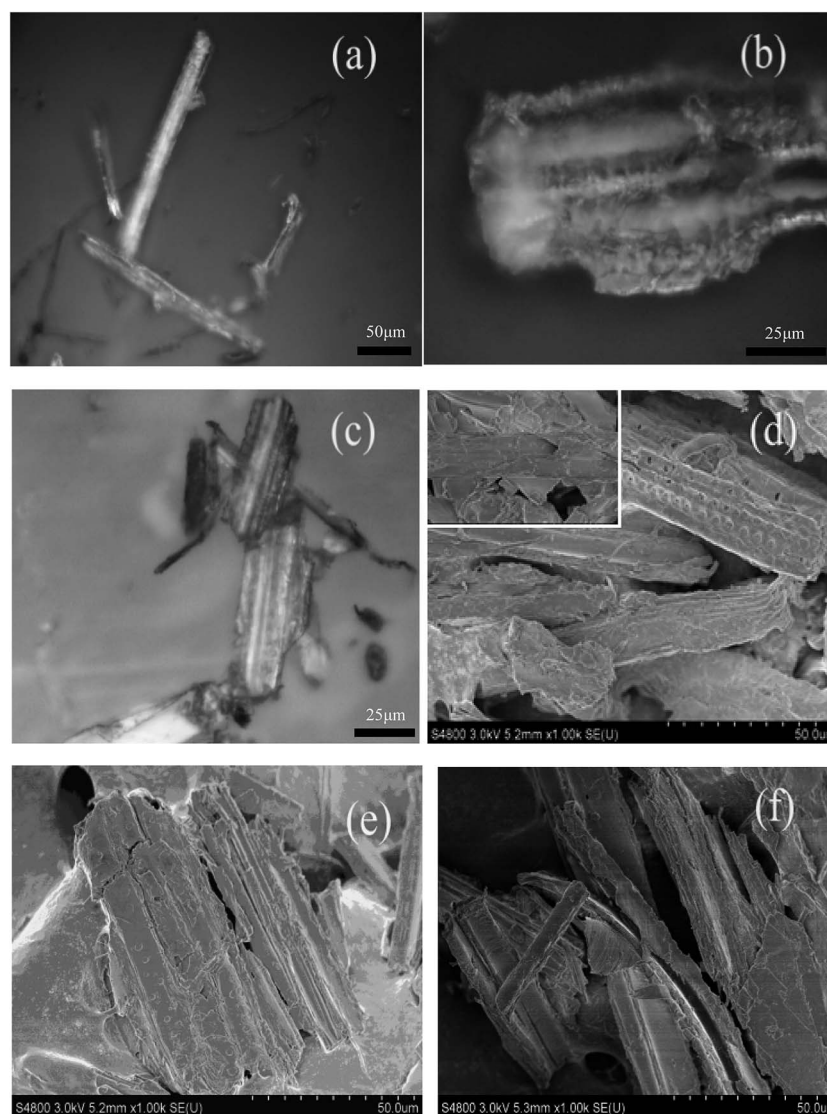


**Table 2** The atomic concentrations and DSS of PA-WS calculated from % P mass concentration

Sample	C 1s (%)	O 1s (%)	N 1s (%)	P 2p (%)	% P mass concentration	DSS
WS	76.55	20.8	2.65			
PA-WS 40 °C	74.19	20.17	2.03	3.61	8.26	0.44
PA-WS 60 °C	64.35	26.46	3.31	5.88	12.78	0.68
PA-WS 80 °C	65.49	26.19	2.33	5.99	13.03	0.70
PA-WS 100 °C	61.05	31.05	5.76	3.18	12.28	0.66
PA-WS 120 °C	60.89	31.45	1.87	5.79	12.45	0.67

(–OH) on the surface of WS provide an outstanding ability to react with phytic acid, and the coarse surface of the WS substrate provides an excellent platform for the high loading of pesticides. From the perspective of PA, the non-toxic phytic acid anchored on the WS substrate offers a large number of active sites for binding IM molecules and endows the PA-WS@IM sample with pH-responsive controlled pesticide-release properties due to the tunable affinity between the phosphate groups

of PA and IM molecules. In brief, the integration of the WS substrate and PA modifier into a single system, in which each component acts in a coordinated way, has directed the critical middle step for the synthesis of the pH-sensitive PA-WS composite. In addition, in contrast to previous mesoporous silica and hydrogel based traditional release systems,<sup>7–9</sup> the as-synthesized PA-WS composites are conducive to large-scale production due to the inexpensive and inexhaustible wheat

**Fig. 3** The optical microscopy images of WS (a), PA-WS (b) and PA-WS@IM (c), and SEM images of WS (d), PA-WS (e) and PA-WS@IM (f).

straw resources. Combining these attributes, this environmentally friendly sustained release system with pH-sensitivity, low cost, and practical applicability for pesticide delivery will be expected to bring significant impact in agricultural fields for pest control.

### 3.2 The pH-dependent release of IM

To evaluate the pH-responsive release properties of the PA-WS carrier, IM was chosen as a model pesticide because of its worldwide and heavy application in agriculture (for over 140 agricultural crops).<sup>37</sup> The test of loading capacity and release behavior of IM was conducted at different initial solution pH, as shown in Fig. 4.

Upon increasing the pH from 2 to 11, the release patterns of IM from the as-prepared PA-WS composites present a decreasing trend, while there was no significant change for the IM release efficiency of WS. Apparently, after PA modification, the PA-WS composites exhibited pH-induced IM release properties. The pH-sensitive release behavior of PA-WS may be attributed to the existence of active phosphate groups generated by the fixation of phytic acid on the WS surface, which provide some additional adsorption sites to effectively bind to IM molecules. This indicates that the PA-WS composite can act as a highly effective platform for pH-triggered IM release, and the level of acidity or alkalinity of the release medium plays an important role in the release capacity of IM. This may be attributed to the variation of surface charge on PA-WS and the different interaction forces between IM and the phosphate groups in the PA-WS composite under varying pH values.<sup>26</sup> More specifically, in a low pH medium, the phosphate functional groups ( $\text{PO}_4^{3-}$ ) are protonated due to the presence of excess hydrogen protons present in the aqueous solution, *i.e.*, the PA-WS is positively-charged, thereby enhancing the electrostatic repulsive forces between the positive IM and PA-WS composite, consequently leading to an increase in the release efficiency. At

higher pH values, the surface charge of PA-WS becomes negative because of the deprotonation of the anionic groups ( $\text{PO}_4^{3-}$ ) in PA-WS, and the increasing counter ions  $\text{OH}^-$  shield the positive charge on the cationic IM molecules.<sup>38</sup> In this case, the electrostatic attraction between PA-WS and IM is dominant, thereby reducing the release amount of IM. From the above analysis, we can obtain a preliminary conclusion that the acidity or alkalinity of the release medium has a great effect on IM release and acidic conditions are more advantageous for IM release.

The above inference can be verified by the point of zero charge ( $\text{pH}_{\text{PZC}}$ ), which is a convenient index of a surface when it becomes either positively or negatively charged as a function of pH.<sup>39</sup> As shown in Fig. 5, the  $\text{pH}_{\text{PZC}}$  of the PA-WS composite was determined to be 6.53. This means the surface of the PA-WS composite was positively charged when  $\text{pH} < 6.53$ , and the electrostatic repulsive forces between PA-WS and IM played a dominate role, promoting the rapid release of the pesticide; the surface of the PA-WS composites was negatively charged when the  $\text{pH} > 6.53$ , and the electrostatic attraction was dominant, which inhibited the IM release. Thereby, the PA modification step endows the PA-WS composite with pH-controlled pesticide release properties. In addition, it can be observed that the  $\text{pH}_{\text{PZC}}$  of WS was determined to be 7.41, which means the surface charge of WS can also be varied by changing the pH of the external medium. However, the IM release properties of WS were pH-independent because of the existence of limited active sites on the WS surface and the relatively low loading capacity (see the inset image in Fig. 4). This further proved that it is necessary to realize pH-sensitive pesticides release properties by modifying WS with phytic acid.

The pH-sensitive release profiles under different time slots were further exploited at various pH values to assess the pH-stimuli response of the IM-loaded PA-WS composites. Several representative pesticide release profiles from the PA-WS@IM composite at  $\text{pH} = 2, 4, 6, 8$  and 10 are shown in Fig. 6, where the percentage of IM released is plotted against time at the designated pH value. As shown in Fig. 6, the release of IM exhibited an evident burst release within 15 min, the process of release reached equilibrium, and the release rate almost had an insignificant increase because it was an immediate process of

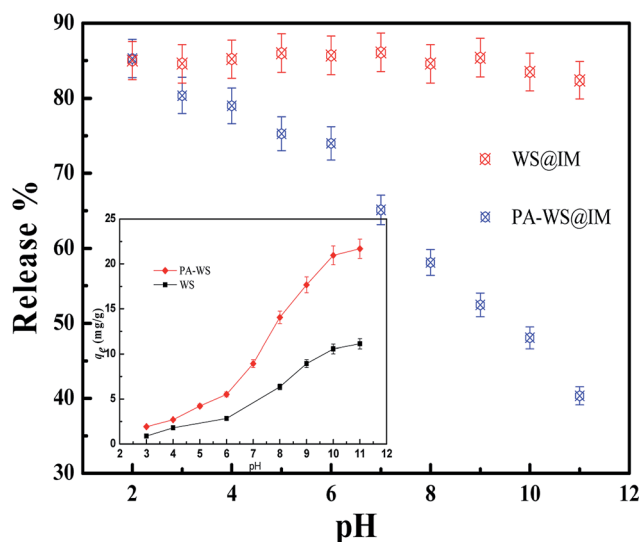


Fig. 4 The effect of the initial pH on the IM release of WS and PA-WS. Inset photographs: the IM loading capacity of WS and PA-WS.

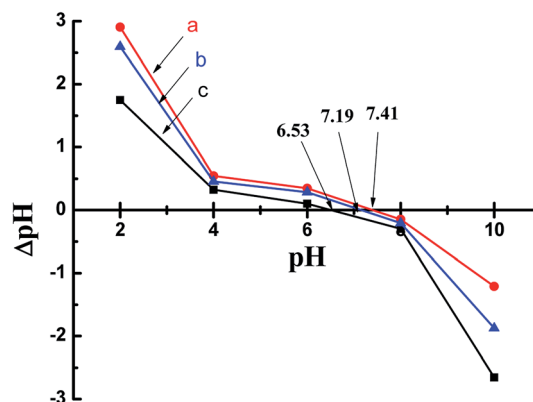


Fig. 5 The  $\text{pH}_{\text{PZC}}$  of WS (a), PA-WS@IM (b) and PA-WS (c).



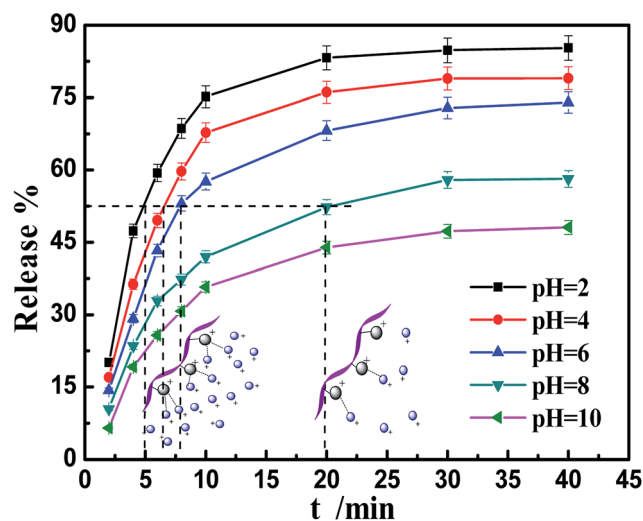


Fig. 6 The cumulative release profiles of IM from the PA-WS@IM composite at different pH values.

protonation of the anionic group ( $\text{PO}_4^{3-}$ ) of PA-WS. Clearly, the pesticide delivery system combined burst-release and sustained-release into a single pesticide carrier, which could achieve sequential release behavior and reduce the frequency of administration, which are of great importance in agriculture, forestry and horticulture fields.

To further shed light on the mechanism of the pH-triggered pesticide delivery system, the experimental data were fitted using the Ritger–Peppas model as expressed in eqn (3):<sup>40</sup>

$$\frac{M_t}{M_\infty} = kt^n \quad (3)$$

where  $M_\infty$  is the initial adsorption capacity of PA-WS, and  $M_t$  is the quantity of IM released at time  $t$ .  $k$  and  $n$  are the system parameters. The fitting curves are shown in Fig. 7. As depicted in Fig. 7, the IM release process was separated into two parts and fitted using the Ritger–Peppas model. The kinetic parameters and correlation coefficients are presented in Table 3. In Table 3, the correlation coefficients ( $R^2$ ) were all over 0.9, indicating a good correlation. In eqn (3), the parameter  $n$  can take

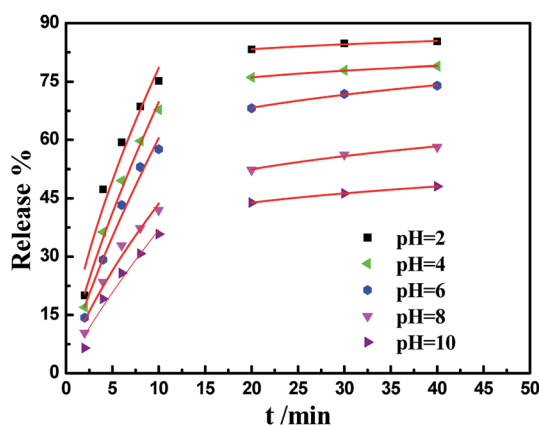


Fig. 7 The Ritger–Peppas model plots of the IM release data.

Table 3 The fitting results of IM release at different pH using the Ritger–Peppas model

	$t < 15 \text{ min}$			$t > 15 \text{ min}$		
	$k$	$n$	$R^2$	$k$	$n$	$R^2$
pH = 2	259.67	0.6669	0.9347	86.68	0.0362	0.9311
pH = 4	272.39	0.7603	0.9796	80.81	0.0543	0.9943
pH = 6	247.03	0.7854	0.9695	77.78	0.1189	0.9917
pH = 8	161.31	0.7293	0.9548	62.09	0.1541	0.9786
pH = 10	163.33	0.8301	0.9533	50.67	0.1308	0.9999

a range of values that indicate the type of transport. When  $0 < n < 0.5$ , the active compound is released by simple Fickian diffusion (stochastic phenomenon), while when  $0.5 < n < 1.0$ , the diffusion process is a combination of Fickian and non-Fickian diffusion, and is known as ‘anomalous diffusion’. Clearly, when  $t < 15 \text{ min}$ ,  $n$  is always greater than 0.5, and when  $t > 15 \text{ min}$ ,  $n$  is always less than 0.5. When  $t < 15 \text{ min}$ , the diffusion process was an ‘anomalous diffusion’ because the break in the ‘membrane’ made the diffusion no longer belong to Fickian diffusion. After 15 min, the structure of the ‘membrane’ was steady and the diffusion belonged to Fickian diffusion.<sup>41</sup> As  $t < 15 \text{ min}$ , the values of  $k$  decreased with an increase in pH because the chemical bonds were easier to cleave under more acidic conditions and consequently, increased the release rate of IM. Shortly, this sustained released system with high adsorption and pH sensitivity was demonstrated to be highly efficient for controllable pesticide delivery with different released rates at different pH values.

### 3.3 The release of IM in the presence of different salt solutions

The IM release properties are often drastically affected by the characteristics of the medium, such as the presence of salt. In order to reflect the properties of IM release under practical conditions, the properties were studied in a medium with the presence of salts, such as  $\text{Na}^+$ ,  $\text{Ca}^{2+}$ , and  $\text{Fe}^{3+}$ , at certain applied concentrations. The results are shown in Fig. 8.

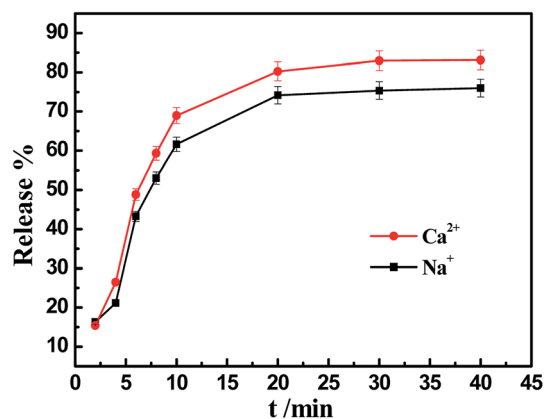


Fig. 8 The effect of saline solutions on the release behavior of PA-WS@IM.



In Fig. 8, solutions of KCl, CaCl<sub>2</sub> and FeCl<sub>3</sub> were utilized to study the properties of IM release at pH 8. Due to the complexation of Fe<sup>3+</sup> ions with IM and the effect of the color of the Fe<sup>3+</sup> ions aqueous solution, the data for the Fe<sup>3+</sup> ions aqueous solution could not be acquired. As depicted in Fig. 8, the efficiency of IM release in a solution of Ca<sup>2+</sup> ions (83.13%) was higher than in the solution of Na<sup>+</sup> ions (75.99%). One factor was that the charge screening effect in the Ca<sup>2+</sup> ion aqueous solution was stronger than that in the Na<sup>+</sup> ion aqueous solution.<sup>42</sup> As a result of the charge screening effect, the effect direction of the negative charges belonging to the phytic acid groups was shifted, and the desorption of IM molecules from the PA-WS surface became easier. Therefore, saline solutions were in favor of the release of IM.

## 4. Conclusions

In summary, a PA-WS composite was successfully synthesized *via* grafting phytic acid onto the surface of WS. IM, as a typical pesticide used in agriculture, was absorbed by PA-WS, and the release mechanism of IM was studied. The FTIR, SEM and zeta potential results proved that the phytic acid molecules were fixed onto the WS surface successfully through an esterification reaction. The degree of substitution (DS) and degree of surface substitution (DSS) indicated that 80 °C was the most favorable temperature for the modification of WS by phytic acid. The results indicated that the dynamic chemical bond between PA-WS and IM can be controlled by adjusting the acidity of the medium, and the release of IM becomes a controllable process. Specifically, the release rate increased upon decreasing the initial medium pH with a maximum release rate of 85.29% in an initial solution at pH 2, and the release kinetics were found to follow the Ritger–Peppas model. Moreover, the release rate of IM in a solution of Ca<sup>2+</sup> ions was higher than in a solution of Na<sup>+</sup> ions. Therefore, PA-WS@IM with simple preparation, low cost and the controllable release capacity shows great potential as a new pesticide release system with pH sensitivity for the reduction of pollution from pesticides.

## Conflict of interest

The authors declare no competing financial interest.

## Acknowledgements

This study was supported by the Project of Qinghai Science and Technology Department (No. 2016-ZJ-Y01), the Fundamental Research Funds for the Central Universities (No. 310829175001), the Open Project of State Key Laboratory of Plateau Ecology and Agriculture, Qinghai University (No. 2017-KF-03) and the National Training Program of Innovation and Entrepreneurship for Undergraduates (No. 201610710070).

## References

- 1 M. Raileanu, L. Todan and M. Crisan, *J. Environ. Prot.*, 2010, **1**, 302–313.
- 2 D. J. Lapworth and D. C. Gooddy, *Environ. Pollut.*, 2006, **144**, 1031–1044.
- 3 P. Palma, M. Kuster and P. Alvarenga, *Environ. Int.*, 2009, **35**, 545–551.
- 4 W. Sheng, S. Ma and W. Li, *RSC Adv.*, 2015, **5**, 13867–13870.
- 5 N. Chen, L. A. Dempere and Z. Tong, *ACS Sustainable Chem. Eng.*, 2016, **4**, 5204–5211.
- 6 W. E. Rudzinski, T. Chipuk and A. M. Dave, *J. Appl. Polym. Sci.*, 2003, **87**, 394–403.
- 7 H. Chen, Y. Lin and H. Zhou, *RSC Adv.*, 2016, **6**, 114714–114721.
- 8 H. Chen, Y. Lin and H. Zhou, *J. Agric. Food Chem.*, 2016, **64**, 8095–8102.
- 9 W. Sheng, S. Ma and W. Li, *RSC Adv.*, 2015, **5**, 13867–13870.
- 10 X. Jia, W. B. Sheng and W. Li, *ACS Appl. Mater. Interfaces*, 2014, **6**, 19552–19558.
- 11 F. Talebnia, D. Karakashev and I. Angelidaki, *Bioresour. Technol.*, 2010, **101**, 4744–4753.
- 12 Y. T. Fan, Y. H. Zhang and S. F. Zhang, *Bioresour. Technol.*, 2006, **97**, 500–505.
- 13 Z. Ma, Q. Li and Q. Yue, *Bioresour. Technol.*, 2011, **102**, 2853–2858.
- 14 I. Bertrand, M. Prevot and B. Chabbert, *Bioresour. Technol.*, 2009, **100**, 155–163.
- 15 N. T. Dunford and J. Edwards, *Bioresour. Technol.*, 2010, **101**, 422–425.
- 16 A. Bhatnagar and M. Sillanpää, *Chem. Eng. J.*, 2010, **157**, 277–296.
- 17 U. S. Orlando, A. U. Baes and W. Nishijima, *Chemosphere*, 2002, **48**, 1041–1046.
- 18 A. K. Mohanty, M. Misra and G. Hinrichsen, *Macromol. Mater. Eng.*, 2000, **276–277**, 1–24.
- 19 S. Jin, J. Chen and J. Mao, *Polym. Compos.*, 2015, 1–10.
- 20 Y. K. Li, B. L. Zhao and L. J. Zhang, *Desalin. Water Treat.*, 2013, **51**, 5735–5745.
- 21 X. F. Sun, Z. Jing and H. Wang, *J. Appl. Polym. Sci.*, 2013, **129**, 1555–1562.
- 22 B. Zhao, Y. Shang and W. Xiao, *J. Environ. Chem. Eng.*, 2014, **2**, 40–45.
- 23 Y. Shang, J. Zhang and X. Wang, *Desalin. Water Treat.*, 2015, **57**, 1–12.
- 24 D. Drobne, M. Blazic and C. A. Van Gestel, *Chemosphere*, 2008, **71**, 1326–1334.
- 25 L. Xie, M. Liu and B. Ni, *Chem. Eng. J.*, 2011, **167**, 342–348.
- 26 H. You, J. Chen and C. Yang, *Colloids Surf., A*, 2016, **509**, 91–98.
- 27 W. J. Liu, F. X. Zeng and H. Jiang, *Bioresour. Technol.*, 2011, **102**, 8247–8252.
- 28 M. Zhang, L. Zhang and P. Chi Keung Cheung, *Biopolymers*, 2003, **26**, 150–159.
- 29 K. Missoum, M. N. Belgacem and J. P. Barnes, *Soft Matter*, 2012, **8**, 8338–8349.
- 30 M. Andresen, L. S. Johansson and B. S. Tanem, *Cellulose*, 2006, **13**, 665–677.
- 31 X. Xu, X. Su and B. Bai, *RSC Adv.*, 2016, **6**, 29880–29888.
- 32 T. Wan, R. Huang and Q. Zhao, *J. Appl. Polym. Sci.*, 2013, **130**, 3404–3410.





- 33 Q. Li, Z. Ma and Q. Yue, *Bioresour. Technol.*, 2012, **118**, 204–209.
- 34 U. Ulusoy, S. Şimşek and Ö. Ceyhan, *Adsorption*, 2003, **9**, 165–175.
- 35 T. Wan, R. Huang and Q. Zhao, *J. Appl. Polym. Sci.*, 2013, **130**, 3404–3410.
- 36 Z. Ma, Q. Li and Q. Yue, *Chem. Eng. J.*, 2011, **171**, 1209–1217.
- 37 D. Drobne, M. Blažič, C. A. M. Van Gestel, V. Lešer, P. Zidar, A. Jemec and P. Trebše, *Chemosphere*, 2008, **71**, 1326–1334.
- 38 T. S. Anirudhan and A. R. Tharun, *Chem. Eng. J.*, 2012, **181**–**182**, 761–769.
- 39 A. E. Ofomaja and Y. S. Ho, *J. Hazard. Mater.*, 2007, **139**, 356–362.
- 40 Z. Wu, Y. He and L. Chen, *Carbohydr. Polym.*, 2014, **110**, 259–267.
- 41 M. Mastromatteo, M. Mastromatteo and A. Conte, *Trends Food Sci. Technol.*, 2010, **21**, 591–598.
- 42 C. I. Diop, H. L. Li and B. J. Xie, *Food Chem.*, 2011, **126**, 1662–1669.

